The Araucaria Project. The Distance of the Large Magellanic Cloud from Near-Infrared Photometry of RR Lyrae Variables [1]

Olaf Szewczyk

Universidad de Concepción, Departamento de Fisica, Astronomy Group, Casilla 160-C, Concepción, Chile

Warsaw University Observatory, Al. Ujazdowskie 4, 00-478, Warsaw, Poland

szewczyk@astro-udec.cl

Grzegorz Pietrzyński

Universidad de Concepción, Departamento de Fisica, Astronomy Group, Casilla 160-C, Concepción, Chile

Warsaw University Observatory, Al. Ujazdowskie 4, 00-478, Warsaw, Poland

pietrzyn@astrouw.edu.pl

Wolfgang Gieren

Universidad de Concepción, Departamento de Fisica, Astronomy Group, Casilla 160-C, Concepción, Chile

wgieren@astro-udec.cl

Jesper Storm

Astrophysikalisches Institut Potsdam, An der Sternwarte 16, D-14482 Potsdam, Germany

jstorm@aip.de

Alistair Walker

Cerro Tololo Inter-American Observatory, Casilla 603, La Serena, Chile

awalker@ctio.noao.edu

Luca Rizzi

Joint Astronomy Centre, 66 N. A'ohoku Pl., Hilo, Hawaii, 96720

luca@ifa.hawaii.edu

Karen Kinemuchi

Universidad de Concepción, Departamento de Fisica, Astronomy Group, Casilla 160-C, Concepción, Chile

University of Florida, Department of Astronomy, Gainesville, Florida 32611-2055, USA

kkinemuchi@astro-udec.cl

Fabio Bresolin

Institute for Astronomy, University of Hawaii at Manoa, 2680 Woodlawn Drive, Honolulu HI 96822, USA

bresolin@ifa.hawaii.edu

Rolf-Peter Kudritzki

Institute for Astronomy, University of Hawaii at Manoa, 2680 Woodlawn Drive, Honolulu HI 96822, USA

kud@ifa.hawaii.edu

Massimo Dall'Ora

INAF, Osservatorio Astronomico di Capodimonte, I-80131 Napoli, Italy

dallora@oacn.inaf.it

ABSTRACT

We have obtained deep infrared J and K band observations of five fields located in the Large Magellanic Cloud (LMC) bar with the ESO New Technology Telescope equipped with the SOFI infrared camera. In our fields, 65 RR Lyrae stars catalogued by the OGLE collaboration were identified. Using different theoretical and empirical calibrations of the period-luminosity-metallicity relation, we find consistent LMC distance moduli values. Since the observed fields are situated very close to the center of the LMC, the correction for the tilt of the LMC bar with respect to the line of sight is negligible. Our adopted best true distance modulus to the LMC of 18.58 ± 0.03 (statistical) $\pm$ 0.11 (systematic) mag agrees very well with most independent determinations to this galaxy.

Subject headings: distance scale - galaxies: distances and redshifts - galaxies: individual(LMC) - stars: RR Lyrae - infrared photometry

1. Introduction

In our ongoing Araucaria Project (e.g. Gieren et al. 2005a), we are applying a number of different stellar standard candles to independently determine the distances to a sample of nearby galaxies. The systematic differences between the distance results obtained for the individual galaxies from the various stellar candles will be analyzed in forthcoming papers. This analysis is expected to finally lead to a detailed understanding of how the various stellar techniques, which are fundamental to calibrate the first rungs of the distance ladder, depend on metallicity and age. While the objects we use for the distance determinations are usually detected from optical wide-field imaging surveys of the target galaxies (e.g. Pietrzyński et al. 2002b), the most accurate distance work is then done from follow-up near-infrared images which virtually eliminate reddening as a significant source of error on the results. Examples of this very successful approach are the recent Cepheid work on NGC 55 (Gieren et al. 2008), and the red clump star work on the LMC (Pietrzyński & Gieren 2002a). The Araucaria Project has also been developing a new spectroscopic distance indicator, viz. the flux-weighted gravity-luminosity relationship for blue supergiants (Kudritzki et al. 2003; 2008) which holds the promise to yield distances accurate to 5% to galaxies containing massive blue stars out to about 10 Mpc from low-resolution spectra.

Thanks to several recent theoretical and empirical studies, evidence has been mounting that RR Lyrae (RRL) stars are excellent standard candles in the near-infrared spectral range, providing distance results which are superior to the traditional optical method (e.g. Bono 2003a). Longmore et al. (1986) were the first to show that RRL variable stars follow a period-luminosity (PL) relation in the near-infrared K-band. Their pioneering work was followed by Liu & Janes (1990), Jones et al. (1996), and Skillen et al. (1993), who applied infrared versions of the Baade-Wesselink method to calibrate the luminosities and distances of RRL stars. A very comprehensive analysis of the IR properties of RRL stars was given by Nemec et al. (1994). The first theoretical constraints on the K-band PL relation of RRL stars are based on non-linear convective pulsation models that were presented by Bono et

[1]Based on observations obtained with the ESO NTT for programme 074.D-0318(B)

al. (2001). Dall'Ora et al. (2004) later demonstrated that the K-band PL relation for RRL stars appears to have a very small scatter for globular clusters, with small intrinsic spread in metallicity for this type of stars. Further theoretical explorations of the RRL period-mean magnitude-metallicity relations in near-infrared passbands were carried out by Bono et al. (2003b), Catelan et al. (2004), and Cassisi et al. (2004). Most recently, Sollima et al. (2006) analyzed near-infrared K-band data of RRL stars in some 15 Galactic globular clusters and provided the first empirical calibration of the period-luminosity-metallicity (PLZ) relation in the K band. All these existing theoretical and empirical studies have suggested that the RRL star K-band PLZ relation appears to be indeed a superb means to determine accurate distances to galaxies hosting an abundant old stellar population.

We have therefore started to include this rather new tool in the Araucaria Project distance work. Pietrzyński et al. (2008) implemented the RRL K-band PLZ relation for single-epoch K-band magnitudes of a large sample of RRL stars in the Sculptor dwarf galaxy. The distance determination from their analysis for this galaxy compares very well with the distance of Sculptor determined from the tip of the red giant branch method. In this paper, we are applying the RRL K-band PLZ relation to a sample of RRL stars in five fields of the Large Magellanic Cloud (LMC). This is especially important because the LMC Cepheid PL relation has served as the fiducial relation to which the Cepheid distances measured to a sample of late-type galaxies by the two HST Key Projects (Freedman et al. 2001; Saha et al. 2001) has been tied. On the other hand, there is still an uncomfortably large and annoying discrepancy among modern distance determinations to the LMC from different methods (e.g. Schaefer 2008; Gieren et al. 2005b; Walker 2003; Feast 2003; Benedict el al. 2002). Most recent distance determinations to the LMC have clustered around the value of 18.5 mag that was adopted by the Key Project (but see a cautionary comment made by Schaefer (2008)). Discrepant results continue to be obtained, as shown by recent exhaustive determinations of Milky Way Cepheid distances from the infrared surface brightness technique (Fouqué et al. 2007; Fouqué & Gieren 1997). A shorter LMC distance modulus (closer to 18.4 mag) was suggested by this method. A first determination of the LMC distance from an application of the K-band PLZ relation on the LMC field RRL variable stars is an important step towards a resolution of the distance discrepancy. This is urgently needed for true progress on the calibration of the distance scale.

2. Observations, Data Reduction and Calibration

All the near-infrared data used and presented in this paper were collected during one of the Araucaria Project observing runs. The SOFI infrared camera of the ESO New Technology

Telescope (NTT) telescope at La Silla Observatory was used. With the Large Field setup we achieved a 4.9×4.9 arcminute field of view and a pixel scale of 0.288 arcsec/pixel.

During two photometric nights we obtained deep Js and Ks observations of five fields in the LMC, with each field containing at least a dozen RRL stars. Fig. 1 displays the location of these fields in the LMC. On the second night, fields 1 and 2 were overlapped with field 3a. Detailed information on each field is given in Table 1. In order to take into consideration the rapid sky level variations in the infrared passband, we used a dithering technique. Total integration times were up to 40 minutes for Ks, and 11 minutes for the Js band.

The pipeline developed in the course of Araucaria Project was used for all the reductions and calibrations. First, the subtraction of sky level was applied in a two-step process which includes the masking of stars with the IRAF xdimsum package (Pietrzyński & Gieren 2002a). Next, each single image was flat fielded and stacked into the final deep field. PSF photometry, including aperture corrections, was performed in the same way as described in Pietrzyński, Gieren & Udalski (2002c).

The calibration of the photometry onto the standard system was based on observations of 14 standard stars from the UKIRT list (Hawarden et al. 2001). All of them were observed together with the target fields during photometric conditions at different airmasses. Thanks to the large number of standard stars observed along with the science target fields, the accuracy of our photometry zero point was estimated to be as good as 0.02 mag. Our calibrated photometric magnitudes were compared with the 2MASS catalogue for common stars, which gave us a zero point difference. Also stars that were measured on both nights and cross-identified on different fields were compared (SC5-FI + SC5-FII with SC5-FIII, and SC7-FV, on following nights). The results of comparison of zero point differences between our work and 2MASS are shown in Table 2. The increase in difference between K-band observations for field 3a may be caused by larger crowding and less accuracy of 2MASS photometry in these regions. The Red Clump (RC) brightness was also compared with previously published data (Pietrzyński, Gieren & Udalski 2003). Results of the determination of the RC star mean brightness in each of our fields are given in Tab. 3. They compare very well with the values found by Pietrzyński & Gieren (2002a) in their observed fields ($J = 17.507 \pm 0.009$, $K = 16.895 \pm 0.007$). The calibrated near-infrared magnitudes for all RRL stars identified in our fields are presented in Tab. 4.

3. Near-Infrared Period-Luminosity Relations

The sample of 65 RRL stars we have observed in our chosen SOFI/NTT fields were cross-identified with the OGLE catalogue of RRL stars in the LMC (Soszyński et al. 2003). The position of all identified stars in the K, $J-K$ color-magnitude diagram is shown on Fig. 2. Most of the stars have only one random-phase measurement, but some have two random-phase observations taken on the two different nights. A few of the RRL stars were cross-identified in the overlapping fields, which provided three measurements for these objects.

The period-luminosity (PL) relations for the J and K bands derived from our data are shown in Fig. 3. For the RRL stars with more than one observation, we took a straight average of the random-phase magnitudes, which should lead to a better approximation of their mean magnitudes. In Fig. 3, two distinct groups can be distinguished that correspond to the first overtone (RRc) and fundamental mode (RRab) pulsators, respectively. The relatively large scatters seen in both figures 2 and 3 is mostly caused by three factors: 1) the random single-phase nature of our IR measurements, which represents the mean magnitude of an RRL variable only to ~ 0.15 mag (e.g. Del Principe et al. 2006), 2) the metallicity spread among RRL stars in the LMC, and 3) the accuracy of our single measurements, which is 0.03-0.19 mag for stars of brightnesses of 16.6-18.6 mag in the K band.

Since the most important contributor to the scatter in Figure 3 is the replacement of the mean magnitudes by single-phase or by averaged few-phase measurements, we used accurate optical (BVI) photometry from the OGLE archive (Soszyński et al. 2003) of the the studied sample of RRL stars, taken close in time to the NIR data. With the additional optical data, we can calculate improved JK phase points in order to use the Jones et al. (1996) template light curve method (available only for the K band). The J, K, and $\langle K \rangle$ magnitudes are given in Table 5.

We compare the PL relations derived for the RRab stars (averaged observations) and for all of the RRL stars (RRab and RRc) against the existing theoretical (Bono et al. 2003b; Catelan et al. 2004) and empirical (Sollima et al. 2006; 2008) relations. Table 6 lists our results for the slope and zero point values of the PL relations as well as those from the theoretical and empirical ones. Furthermore, in Table 7, we present the K-band zero point and slope values obtained from $\langle K \rangle$ magnitudes derived from the Jones et al. (1996) light curve template method.

4. The Distance Determination

In order to derive the apparent distance moduli to LMC from our data, we used the following calibrations of the near-infrared PL relations of mixed population RRL stars:

$$M_K = -1.07 - 2.38 \log P + 0.08[Fe/H] \quad \text{– Sollima et al. (2008)} \tag{1}$$

$$M_K = -0.77 - 2.101 \log P + 0.231[Fe/H] \quad \text{– Bono et al. (2003b)} \tag{2}$$

$$M_K = -0.597 - 2.353 \log P + 0.175 \log Z \quad \text{– Catelan et al. (2004)} \tag{3}$$

$$M_J = -0.141 - 1.773 \log P + 0.190 \log Z \quad \text{– Catelan et al. (2004)} \tag{4}$$

We recall that the calibration of Sollima et al. (2008) was constructed for the 2MASS photometric system, while the calibrations of Catelan et al. (2004) and Bono et al. (2003b) are valid for the Glass and Bessel and Brett systems, respectively. Therefore, we transformed our own data, calibrated onto the UKIRT system (Hawarden et al. 2001) to the Glass and Bessel and Brett systems using the transformations given by Carpenter (2001) before calculating distances using the calibrations of Catelan et al. (2004) and Bono et al. (2003b). Since there is virtually no difference between the K-band of 2MASS and UKIRT (Carpenter 2001), we did not apply any transformations to our data while using the Sollima et al. (2008) calibration.

In order to combine the RRab and RRc stars, we fundamentalize the RRc periods by adding $\log P = 0.127$. Assuming the mean metallicity of our RRL sample to be $[Fe/H] = -1.48$ (Gratton et al. 2004), we have calculated the K and J band distance moduli for the averaged magnitude and mean magnitude based on the template light-curve data. The fits for the relations 1-4 to both sets of data are displayed in Figs 4 and 5.

To correct the derived apparent distance moduli for interstellar reddening, we adopted reddening maps of $E(B-V)$ calculated for the LMC by Udalski et al. (1999). Assuming the reddening law from Fitzpatrick (1999), we calculate the following selective extinctions in the different bands: $A_K = 0.367E(B-V)$ and $A_J = 0.902E(B-V)$.

For the averaged K band data the true distance moduli of 18.58 ± 0.03, 18.62 ± 0.03, and 18.60 ± 0.03 mag, were obtained using the calibrations of Sollima et al. (2008), Bono et al (2003b) and Catelan et al. (2004), respectively. Based on the J band data and the calibration

of Catelan et al. (2004), the distance moduli of 18.55 ± 0.03 mag was derived. Similar values of the true distance moduli were calculated using the mean $\langle K \rangle$ band magnitudes obtained from the Jones et al. (1996) template fitting (18.56 ± 0.03 - Sollima et al. (2008), 18.60 ± 0.03 - Bono et al. (2003b), 18.59 ± 0.03 - Catelan et al. (2004)). These results are summarized in Tab. 8. For our best distance determination, we adopt the average value from all the results to be of 18.58 ± 0.03 mag.

5. Discussion

The distance moduli obtained based on several independent theoretical and empirical calibrations are consistent. The maximum difference of 0.04 mag between the results from the calibrations of Sollima et al. (2008) and Bono et al. (2003b) is certainly not significant taking into account all uncertainties, which affect the whole process of constructing the mentioned calibrations. However, it is interesting to note that a very similar difference between the distance moduli derived using these two calibrations was recently obtained by Pietrzyński et al. (2008) for the Sculptor galaxy ($[Fe/H] = -1.83$ dex). Therefore, perhaps there is just a zero point offset in the sense that the distances from the calibration of Sollima et al. (2008) are slightly shorter compared to those from the calibration of Bono et al. (2003b).

Taking into account the errors associated with the adopted calibrations, mean metallicity, photometric zero point and absorption correction, we estimate the systematic error of our distance determination to be of 0.11 mag. Therefore our best distance modulus determination to the LMC is: 18.58 ± 0.03 (statistical) ± 0.11 (systematic) mag.

It is worthwhile to mention that the observed fields are located not only close to the LMC center, but also opposite each other around it, so the corrections for the tilt of this galaxy with respect to the line of sight are expected to be very small. Indeed applying the geometrical model of van der Marel et al. (2002) to correct our data for this effect, we obtain a distance modulus shorter by 0.01 mag. Comparing our distance result from the present field RR Lyrae stars to the distance obtained by Dall'Ora el al. (2004) for the Reticulum cluster, there is evidence that the cluster could be very slightly nearer than the LMC center, by about 3%, but this small difference is clearly within the combined uncertainties, even the statistical ones, of both determinations.

Very recently Sollima et al. (2008), using their calibration and the IR data of a sample of RRL stars presented by Borissova et al. (2004), obtained a distance modulus to the LMC of 18.56 ± 0.13 mag. Our distance moduli derived based on this same calibration are virtually the same, which reinforces both results.

Our distance modulus agrees very well with the most LMC distance moduli derived from other independent techniques (Freedman et al. 2001; Benedict et al. 2002; Walker 2003). In particular this result is very similar to the measurements obtained based on the near infrared photometry of Cepheids (Persson et al. 2004) and the red clump stars (Alves et al. 2002; Grocholski & Sarajedini 2002; Pietrzyński & Gieren 2002a).

6. Summary and Conclusions

The results of our deep infrared imaging of 65 RR Lyrae stars in the central regions of the LMC are presented. Our data shows two clear sequences in the period luminosity plane, which correspond to the RRc and RRab stars. After fundamentalizing the RRc periods to the period of the RRab stars by adding $\log P = 0.127$, both groups were merged, and the distance moduli to the LMC were determined using different theoretical and empirical calibrations. Our final adopted distance agrees very well with the recent results obtained from the near infrared observations of Cepheids and red clump stars as well as with those calculated from other techniques.

Our results confirm that the RR Lyrae period-luminosity-metallicity relations in the near infrared passband are potentially a very good tool for precise distance measurements.

WG and GP gratefully acknowledge financial support for this work from the Chilean Center for Astrophysics FONDAP 15010003. Support from the Polish grant N203 002 31/046 and the FOCUS subsidy of the Fundation for Polish Science (FNP) is also acknowledged. WG gratefully acknowledges support for this work from the Chilean Centro de Astrofisica y Tecnologias Afines, CATA. It is a special pleasure to thank the support astronomers at ESO-La Silla for their expert help in the observations, and the ESO OPC for the generous amounts of observing time at the NTT allocated to our programme. We thank the referee, Dr. Giuseppe Bono, for constructive remarks which helped to improve the paper.

REFERENCES

Alves, D., Rejkuba, M., Minniti, D. & Cook, K., 2002, ApJ, 573, L51

Benedict, G.F., et al., 2002, AJ, 124, 1695

Bono, G., Caputo, F., Castellani, V., Marconi, M. & Storm, J., 2001, MNRAS, 326, 1183

Bono, G., 2003a, in Stellar Candles for the Extragalactic Distance Scale, eds. D. Alloin and W. Gieren, Lecture Notes in Physics, Vol. 635, p. 85

Bono, G., Caputo, F., Castellani, V., Marconi, M., Storm, J. & Degl'Innocenti, S., 2003b, MNRAS, 344, 1097

Borrisova, J., Minniti, D., Rejkuba, M., Alves, D., Cook, K.H. & Freeman, K.C., 2004, A&A, 423, 97

Carpenter, J.M., 2001, AJ, 121, 2851

Cassisi, S., Castellani, M., Caputo, F. & Castellani, V., 2004, A&A, 426, 641

Catelan, M., Pritzl, B.J. & Smith, H.A., 2004, ApJS, 154, 633

Dall'Ora, M., Storm, J., Bono, G., et al., 2004, ApJ, 610, 269

Del Principe, M., Piersimoni, A.M., Storm, J., et al., 2006, ApJ, 652, 362

Feast, M.W., 2003, in Stellar Candles for the Extragalactic Distance Scale, eds. D. Alloin and W. Gieren, Lecture Notes in Physics, Vol. 635, p. 45

Fitzpatrick, E.L., 1999, PASP, 111, 63

Fouqué, P., and Gieren, W., 1997, A&A, 320, 799

Fouqué, P., Arriagada, P., Storm, J., et al., 2007, A&A, 476, 73

Freedman, W.L., et al., 2001, ApJ, 553, 47

Gieren, W., Pietrzyński, G., Bresolin, F., et al., 2005a, Messenger, 121, 23

Gieren, W., Storm, J., Barnes, T.G., Fouqué, P., Pietrzyński, G. & Kienzle, F., 2005b, ApJ, 627, 224

Gieren, W., Pietrzyński, G., Soszyński, I., Bresolin, F., Kudritzki, R.P., Storm, J. & Minniti, D., 2008, ApJ, 672, 266

Gratton, R.G., Bragaglia, A., Clementini, G., Caretta, E., Di Fabrizio, L., Maio, K. & Taribello, E., 2004, A&A, 421, 937

Grocholski, A.,J., and Sarajedini, A., 2002, AJ, 123, 1603

Hawarden, T.G., Leggett, S.K., Letawsky, M.B., et al., 2001, MNRAS, 325, 563

Jones, R.V., Carney, B.W. & Fulbright, J.P., 1996, PASP, 108, 877

Kudritzki, R.-P., Bresolin, F. & Przybilla, N., 2003, ApJ, 582, L83

Kudritzki, R.-P., Urbaneja, M.A., Bresolin, F., Przybilla, N., Gieren, W. & Pietrzyński, G., 2008, ApJ, submitted, astro-ph/arXiv0803.3654

Liu, T., and Janes, K.A., 1990, ApJ, 354, 273

Longmore, A.J., Fernley, J.A. & Jameson, R.F., 1986, MNRAS, 220, 279

Nemec, J.M., Nemec, A.F. Linnell & Lutz, T.E., 1994, AJ, 108, 222

Persson, S.E., Madore, B.F., Krzemiński, W., Freedman, W.L., Roth, M. & Murphy, D.C., 2004, AJ, 128, 2239

Pietrzyński, G., and Gieren, W., 2002a, AJ, 124, 2633

Pietrzyński, G., Gieren, W., Fouqué, P. & Pont, F., 2002b, AJ, 123, 789

Pietrzyński, G., Gieren, W. & Udalski, A., 2002c, PASP, 114, 298

Pietrzyński, G., Gieren, W. & Udalski, A., 2003, AJ, 125, 2494

Pietrzyński, G., Gieren, W., Szewczyk, O., Rizzi, L., Bresolin, F., Kudritzki, R.-P., Nalewajko, K., Storm, J., Dall'Ora, M. & Ivanov, V., 2008, AJ, submitted

Saha, A., Sandage, A., Tammann, G.A., Dolphin, A.E., Christensen, J., Panagia, N. & Maccetto, F.D., 2001, ApJ, 550, 554

Schaefer, B.E., 2008, AJ, in press, astro-ph/arXiv0709.4531

Skillen, I., Fernley, J.A., Stobie, R.S. & Jameson, R.F., 1993, MNRAS, 265, 301

Sollima, A., Cacciari, C. & Valenti, E., 2006, MNRAS, 372, 1675

Sollima, A., Cacciari, C., Arkharov, A.A., Larionow, V.M., Gorshanov, N.V. & Piersimoni, A., 2008, MNRAS, in press, astro-ph/arXiv0712.0578

Soszyński, I., Udalski, A., Szymański, M., Kubiak, M., Pietrzyński, G., Woźniak, P., Żebruń, K., Szewczyk, O. & Wyrzykowski, Ł, 2003, Acta Astronomica, 53, 93

Udalski, A., Soszyński, I., Szymański, M., Kubiak, M., Pietrzyński, G. Woźniak, P. & Żebruń, K., 1999, Acta Astronomica, 49, 223

Van der Marel, R.P., Alves, D.R., Hardy, E. & Suntzeff, N.B., 2002, AJ, 124, 2639

Walker, A.R., 2003, in Stellar Candles for the Extragalactic Distance Scale, eds. D. Alloin and W. Gieren, Lecture Notes in Physics, Vol. 635, p. 265

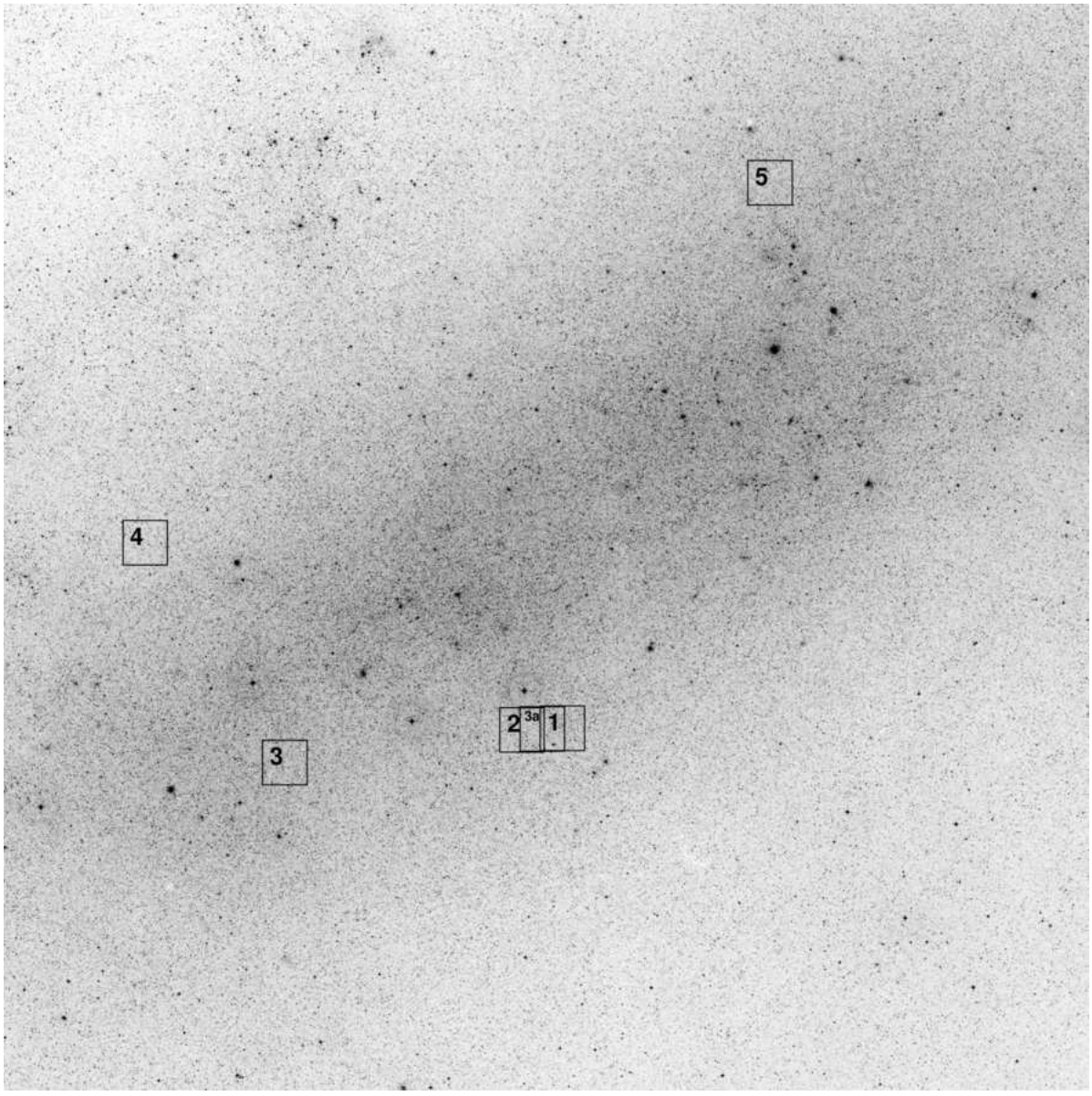

Fig. 1.— The location of our observed 5×5 arcmin NTT/SOFI fields in LMC on the DSS-2 infrared plate. North is up and east to the left.

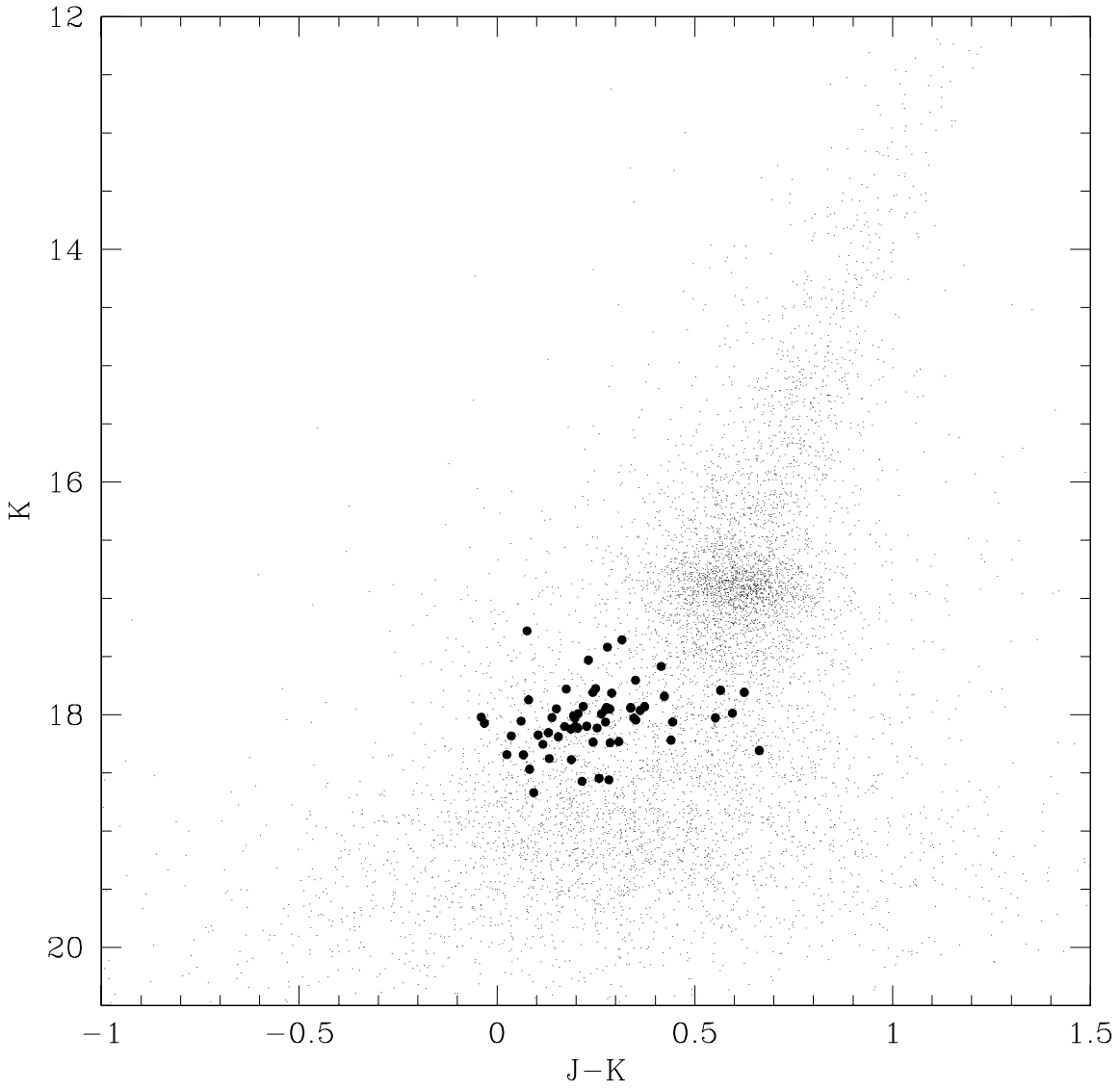

Fig. 2.— The color-magnitude diagram showing identified RR Lyrae stars (filled circles) in observed fields .

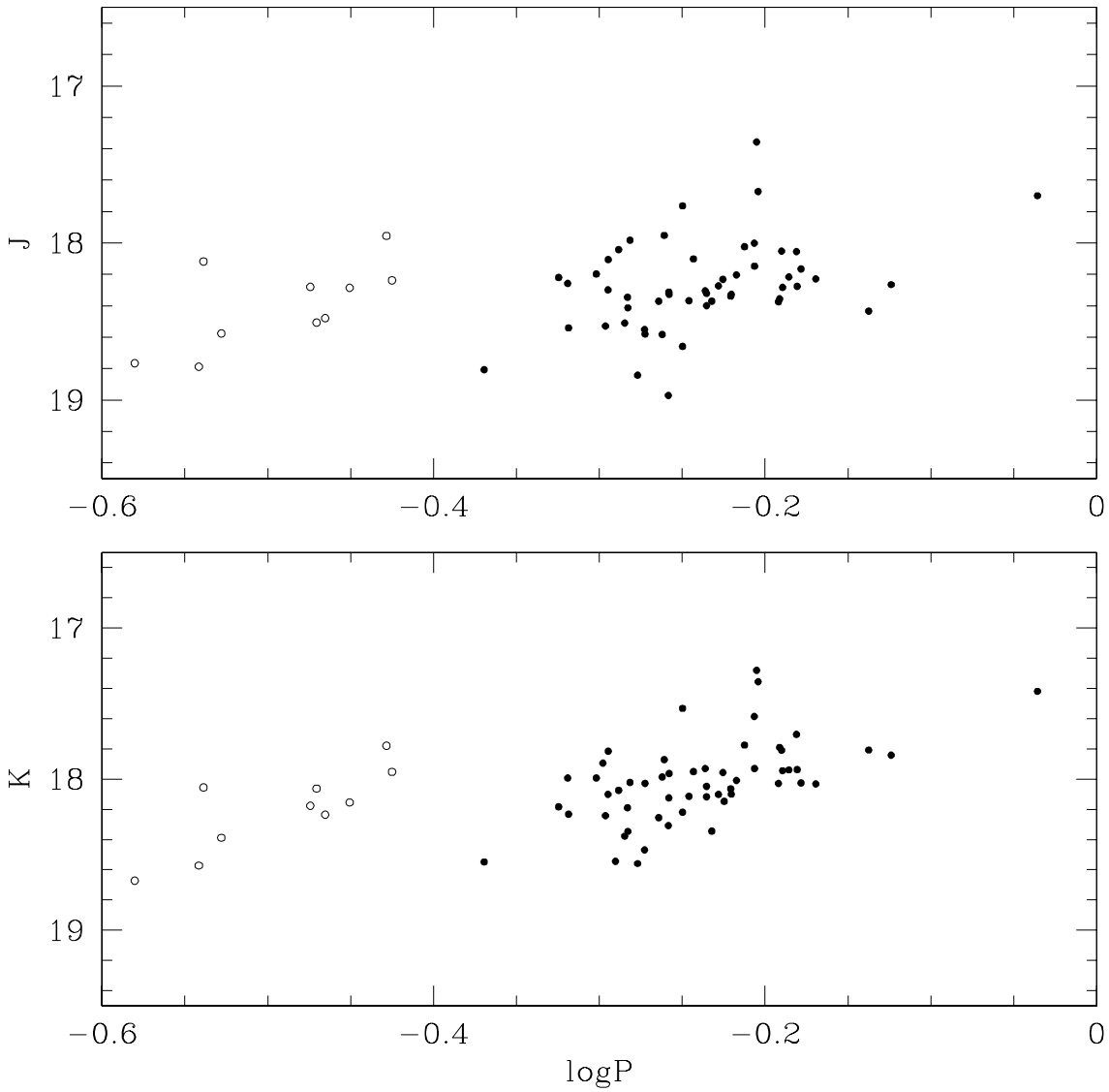

Fig. 3.— The near-infrared K and J band period-luminosity relations defined by the 65 RR Lyrae stars observed in LMC. Period is in days. Two distinct groups are formed by the fundamental (filled circles) and first overtone (open circles) pulsators which are clearly seen in each panel.

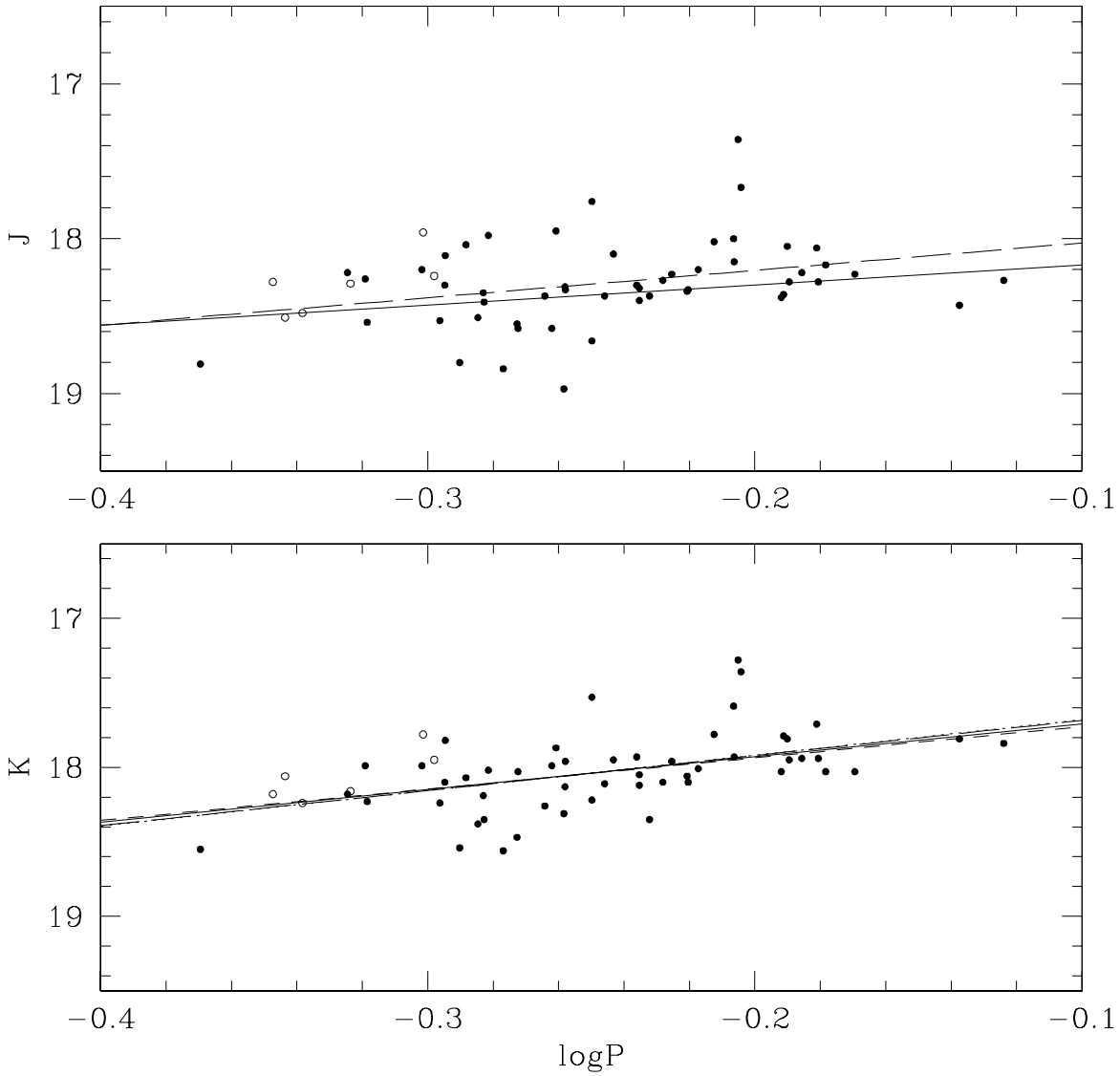

Fig. 4.— The near-infrared PL relations in K and J defined by our RR Lyrae sample in LMC, plotted along with the best-fitting lines. The slopes of the fits were adopted from the recent theoretical and empirical calibrations, and the zero points determined from our data. The solid, dotted, short and long dashed lines correspond to free fit and the calibration of Sollima et al. (2008), Bono et al. (2003), and Catelan et al. (2004), respectively.

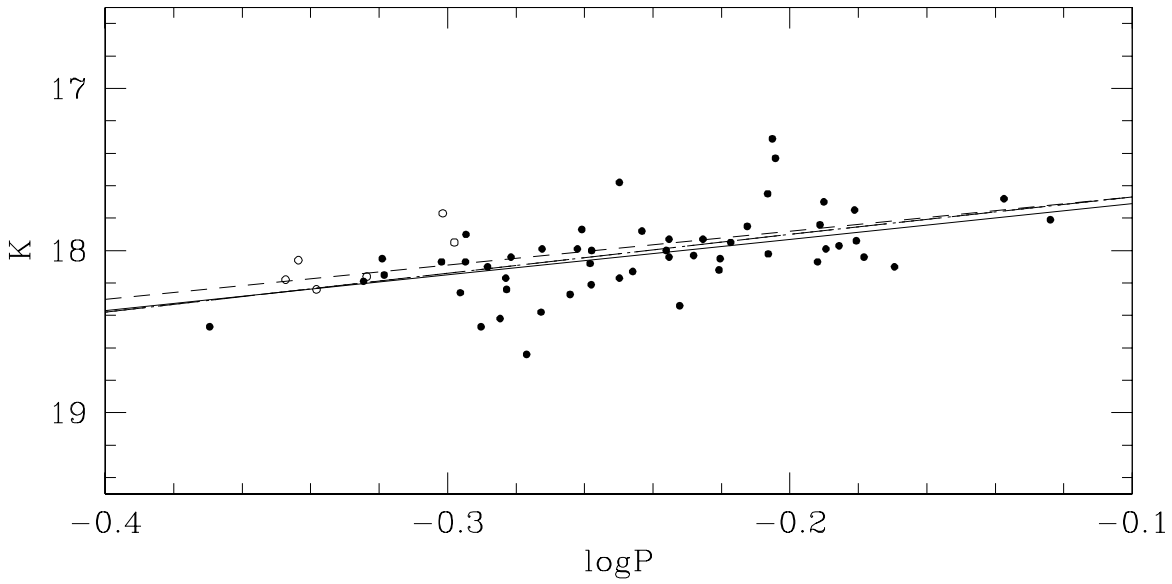

Fig. 5.— The near-infrared PL relations in $\langle K \rangle$ band (corrected with light-curve templates) defined by our RR Lyrae sample in LMC, plotted along with the best-fitting lines. The slopes of the fits were adopted from the recent theoretical and empirical calibrations, and the zero points determined from our data. The solid, dotted, short and long dashed lines correspond to free fit and the calibration of Sollima et al. (2008), Bono et al. (2003), and Catelan et al. (2004), respectively.

Table 1. Observational information of the target fields. Extinction values based on reddening maps by Udalski et al. (1999).

Field No	Field name	RA2000	DEC2000	Date of observation	Extinction E(B-V)
1	SC5-FI	05:23:24.0	-70:05:24.0	2006-09-22	0.130
2	SC5-FII	05:24:16.7	-70:05:24.0	2006-09-22	0.130
3a	SC5-FIII	05:23:50.3	-70:05:24.0	2007-04-06	0.130
3	SC3-FIII	05:29:26.3	-70:07:30.0	2007-04-06	0.134
4	SC2-FIV	05:32:05.0	-69:42:12.9	2007-04-06	0.150
5	SC7-FV	05:18:38.4	-69:06:00.0	2006-09-22, 2007-04-06	0.146

Table 2. Difference of zeropoint estimation between 2MASS and observed data.

Field No	Field name	2mass-j20070406	2mass-k20070406
3a	SC5-FIII	0.03 ± 0.13	0.13 ± 0.30
3	SC3-FIII	0.00 ± 0.10	0.02 ± 0.10
4	SC2-FIV	0.09 ± 0.15	0.03 ± 0.11
5	SC7-FV	0.09 ± 0.13	0.01 ± 0.11

Table 3. Comparison of red clump star brightnesses for the observed fields.

Field	Date	J RC	K RC
1 SC5-FI	2006-09-22	17.358±0.011	16.895±0.006
2 SC5-FII	2006-09-22	17.504±0.006	16.950±0.004
3a SC5-FIII	2007-04-06	17.437±0.009	16.917±0.007
3 SC3-FIII	2007-04-06	17.492±0.014	16.900±0.007
4 SC2-FIV	2007-04-06	17.459±0.012	16.924±0.006
5 SC7-FV	2006-09-22	17.510±0.009	16.956±0.007
5 SC7-FV	2007-04-06	17.505±0.012	16.950±0.008

Table 4. Individual J and K band Observations of RR Lyrae stars in LMC fields

Star ID	Star type	Field name	J HJD +2400000	J mag	σ	K HJD +2400000	K mag	σ
OGLE051817.95-690358.9	ab	LMC-SC7-FV	54001.30645	18.84	0.05	54001.31523	18.44	0.06
			54196.98138	18.78	0.06	54196.98915	18.66	0.12
OGLE051818.33-690513.2	c	LMC-SC7-FV	54001.30645	18.31	0.04	54001.31523	18.17	0.05
			54196.98138	18.26	0.07	54196.98915	18.14	0.07
OGLE051818.71-690506.2	ab	LMC-SC7-FV	54001.30645	17.73	0.03	54001.31523	17.42	0.03
			54196.98138	17.61	0.04	54196.98915	17.30	0.05
OGLE051820.31-690819.4	c	LMC-SC7-FV	54001.30645	18.10	0.06	54001.31523	18.10	0.05
			54196.98138	18.13	0.06	54196.98915	18.02	0.08
OGLE051824.42-690459.4	ab	LMC-SC7-FV	54001.30645	18.40	0.04	54001.31523	18.08	0.04
			54196.98138	18.17	0.04	54196.98915	17.81	0.06
OGLE051834.72-690550.6	ab	LMC-SC7-FV	54001.30645	18.15	0.04	54001.31523	17.97	0.04
			54196.98138	18.25	0.04	54196.98915	18.02	0.07
OGLE051835.56-690406.0	ab	LMC-SC7-FV	54001.30645	18.20	0.05	54001.31523	18.09	0.05
			54196.98138	18.24	0.06	54196.98915	18.28	0.08
OGLE051836.59-690839.6	ab	LMC-SC7-FV	54001.30645	18.55	0.09	54001.31523	18.47	0.05
OGLE051836.68-690659.7	ab	LMC-SC7-FV	54001.30645	18.27	0.07	54001.31523	18.10	0.04
OGLE051837.86-690821.3	c	LMC-SC7-FV	54001.30645	18.80	0.07	54001.31523	18.57	0.06
			54196.98138	18.77	0.06	54196.98915	18.57	0.10
OGLE051841.62-690609.4	ab	LMC-SC7-FV	54001.30645	18.36	0.03	54001.31523	17.87	0.04
			54196.98138	18.17	0.04	54196.98915	17.81	0.06
OGLE051842.24-690724.5	ab	LMC-SC7-FV	54001.30645	18.28	0.03	54001.31523	17.94	0.03
OGLE051843.33-690502.6	ab	LMC-SC7-FV	54001.30645	18.43	0.05	54001.31523	18.14	0.05

Table 4—Continued

Star ID	Star type	Field name	J HJD +2400000	J mag	σ	K HJD +2400000	K mag	σ
			54196.98138	18.31	0.05	54196.98915	18.09	0.07
OGLE051853.07-690819.5	ab	LMC-SC7-FV	54196.98138	18.30	0.04	54196.98915	17.93	0.06
OGLE051923.06-693859.0	ab	LMC-SC7-FV	54001.30645	18.36	0.05	54001.30645	17.80	0.07
			54196.98138	18.35	0.07	54196.98915	17.79	0.07
OGLE052301.40-700731.0	c	LMC-SC5-FI	54001.21410	18.58	0.05	54001.22293	18.39	0.05
OGLE052308.89-700746.7	c	LMC-SC5-FI	54001.21410	18.48	0.05	54001.22293	18.24	0.05
OGLE052317.13-700607.2	ab	LMC-SC5-FI	54001.21410	18.33	0.08	54001.22293	18.10	0.08
OGLE052318.43-700651.5	ab	LMC-SC5-FI	54001.21410	18.33	0.05	54001.22293	17.96	0.04
OGLE052321.67-700739.9	ab	LMC-SC5-FI	54001.21410	18.41	0.06	54001.22293	18.35	0.04
OGLE052328.70-700523.8	c	LMC-SC5-FI	54001.21410	18.13	0.08	54001.22293	17.83	0.07
		LMC-SC5-FIII	54196.99858	17.78	0.05	54197.00711	17.73	0.07
OGLE052329.54-700713.1	ab	LMC-SC5-FI	54001.21410	17.90	0.04	54001.22293	17.66	0.03
		LMC-SC5-FIII	54196.99858	18.21	0.08	54197.00711	17.75	0.05
OGLE052331.40-700529.1	ab	LMC-SC5-FI	54001.21410	17.92	0.06	54001.22293	17.79	0.04
		LMC-SC5-FIII	54196.99858	18.12	0.07	54197.00711	17.76	0.08
OGLE052332.28-700654.1	ab	LMC-SC5-FI	54001.21410	17.35	0.03	54001.22293	17.28	0.03
		LMC-SC5-FIII	54196.99858	17.37	0.05	54197.00711	17.29	0.05
OGLE052335.14-700505.4	ab	LMC-SC5-FI	54001.21410	18.21	0.05	54001.22293	18.06	0.04
		LMC-SC5-FIII	54196.99858	18.39	0.05	54197.00711	18.14	0.08
OGLE052340.40-700639.8	ab	LMC-SC5-FIII	54196.99858	18.04	0.07	54197.00711	18.07	0.08
OGLE052341.81-700632.4	ab	LMC-SC5-FI	54001.21410	18.97	0.11	54001.22293	18.80	0.07
		LMC-SC5-FIII	54196.99858	18.69	0.05	54197.00711	18.32	0.09

Table 4—Continued

Star ID	Star type	Field name	J HJD +2400000	J mag	σ	K HJD +2400000	K mag	σ
OGLE052345.86-700504.2	ab	LMC-SC5-FI	54001.21410	17.85	0.05	54001.22293	17.79	0.06
		LMC-SC5-FIII	54196.99858	18.35	0.05	54197.00711	18.11	0.08
OGLE052349.66-700327.1	ab	LMC-SC5-FI	54001.21410	18.08	0.07	54001.22293	17.83	0.06
		LMC-SC5-FII	54001.26192	18.15	0.07	54001.27070	18.23	0.07
		LMC-SC5-FIII	54196.99858	18.27	0.07	54197.00711	18.02	0.08
OGLE052350.37-700443.2	ab	LMC-SC5-FI	54001.21410	18.50	0.07	54001.22293	18.22	0.06
		LMC-SC5-FII	54001.26192	18.61	0.05	54001.27070	18.26	0.05
		LMC-SC5-FIII	54196.99858	18.48	0.05	54197.00711	18.25	0.09
OGLE052353.56-700432.4	ab	LMC-SC5-FII	54001.26192	18.44	0.04	54001.27070	18.22	0.04
		LMC-SC5-FIII	54196.99858	18.18	0.05	54197.00711	18.03	0.07
OGLE052355.34-700802.6	c	LMC-SC5-FII	54001.26192	18.82	0.08	54001.27070	18.54	0.06
		LMC-SC5-FIII	54196.99858	18.71	0.08	54197.00711	18.81	0.18
OGLE052357.93-700322.9	ab	LMC-SC5-FII	54001.26192	...	...	54001.27070	18.56	...
		LMC-SC5-FIII	54196.99858	18.80	0.08	54197.00711	18.53	0.12
OGLE052400.52-700520.9	ab	LMC-SC5-FII	54001.26192	18.40	0.03	54001.27070	17.98	0.04
		LMC-SC5-FIII	54196.99858	18.40	0.04	54197.00711	18.12	0.07
OGLE052405.11-700611.5	ab	LMC-SC5-FII	54001.26192	18.18	0.04	54001.27070	17.92	0.05
		LMC-SC5-FIII	54196.99858	18.29	0.06	54197.00711	17.99	0.07
OGLE052418.64-700307.7	c	LMC-SC5-FIII	54196.99858	18.28	0.11	54197.00711	18.18	0.16
OGLE052419.91-700616.7	ab	LMC-SC5-FII	54001.26192	...	...	54001.27070	17.90	...
OGLE052423.93-700736.4	ab	LMC-SC5-FII	54001.26192	18.32	0.05	54001.27070	18.12	0.04
OGLE052859.00-700822.2	ab	LMC-SC3-FIII	54197.01705	18.97	0.10	54197.02559	18.31	0.13

Table 4—Continued

Star ID	Star type	Field name	J HJD +2400000	J mag	σ	K HJD +2400000	K mag	σ
OGLE052909.42-700828.1	ab	LMC-SC3-FIII	54197.01705	17.70	0.05	54197.02559	17.42	0.07
OGLE052911.54-700836.5	ab	LMC-SC3-FIII	54197.01705	18.58	0.06	54197.02559	17.99	0.07
OGLE052917.43-700734.5	ab	LMC-SC3-FIII	54197.01705	18.34	0.04	54197.02559	18.06	0.07
OGLE052917.77-700535.6	ab	LMC-SC3-FIII	54197.01705	18.43	0.07	54197.02559	17.81	0.07
OGLE052917.87-700841.1	ab	LMC-SC3-FIII	54197.01705	18.54	0.05	54197.02559	18.23	0.08
OGLE052917.92-700712.2	c	LMC-SC3-FIII	54197.01705	18.51	0.07	54197.02559	18.06	0.10
OGLE052929.39-700551.0	ab	LMC-SC3-FIII	54197.01705	18.00	0.04	54197.02559	17.59	0.06
OGLE052932.88-700842.3	ab	LMC-SC3-FIII	54197.01705	18.37	0.06	54197.02559	18.26	0.09
OGLE052933.54-700715.9	ab	LMC-SC3-FIII	54197.01705	18.58	0.05	54197.02559	18.03	0.08
OGLE052936.94-700721.1	ab	LMC-SC3-FIII	54197.01705	18.37	0.05	54197.02559	18.35	0.08
OGLE052937.91-700844.9	c	LMC-SC3-FIII	54197.01705	18.24	0.05	54197.02559	17.95	0.08
OGLE052949.93-700558.2	ab	LMC-SC3-FIII	54197.01705	18.66	0.06	54197.02559	18.22	0.09
OGLE053147.30-694349.6	ab	LMC-SC2-FIV	54197.04702	18.11	0.05	54197.05671	17.82	0.07
OGLE053147.82-694142.2	ab	LMC-SC2-FIV	54197.04702	18.05	0.05	54197.05671	17.81	0.07
OGLE053155.92-694232.4	ab	LMC-SC2-FIV	54197.04702	18.35	0.05	54197.05671	18.19	0.08
OGLE053200.94-694219.1	ab	LMC-SC2-FIV	54197.04702	18.20	0.09	54197.05671	18.01	0.12
OGLE053203.62-694210.7	ab	LMC-SC2-FIV	54197.04702	18.26	0.04	54197.05671	17.99	0.07
OGLE053206.72-694342.1	ab	LMC-SC2-FIV	54197.04702	18.51	0.04	54197.05671	18.38	0.09
OGLE053206.78-694224.7	ab	LMC-SC2-FIV	54197.04702	17.98	0.04	54197.05671	18.02	0.07
OGLE053207.32-694117.2	ab	LMC-SC2-FIV	54197.04702	17.76	0.03	54197.05671	17.53	0.06
OGLE053207.88-694058.7	ab	LMC-SC2-FIV	54197.04702	18.15	0.04	54197.05671	17.93	0.07
OGLE053217.55-694317.6	ab	LMC-SC2-FIV	54197.04702	17.95	0.08	54197.05671	17.87	0.07

Table 4—Continued

Star ID	Star type	Field name	J HJD +2400000	J mag	σ	K HJD +2400000	K mag	σ
OGLE053219.15-694215.2	ab	LMC-SC2-FIV	54197.04702	18.22	0.05	54197.05671	17.94	0.07
OGLE053222.39-693952.9	ab	LMC-SC2-FIV	54197.04702	18.23	0.07	54197.05671	18.03	0.11
OGLE053225.42-694438.2	ab	LMC-SC2-FIV	54197.04702	18.38	0.07	54197.05671	18.03	0.12
OGLE053229.21-694411.0	ab	LMC-SC2-FIV	54197.04702	...	...	54197.05671	18.15	0.09

Table 5. Averaged and mean magnitudes based on K-band template light-curves of RR Lyrae stars.

Star ID	Star type	Period [days]	J	σ	K	σ	$\langle K \rangle$	σ
OGLE051817.95-690358.9	ab	0.4270819	18.81	0.08	18.55	0.13	18.47	0.08
OGLE051818.33-690513.2	c	0.3543007	18.29	0.08	18.16	0.09	18.16	0.02
OGLE051818.71-690506.2	ab	0.6248463	17.67	0.05	17.36	0.06	17.43	0.05
OGLE051820.31-690819.4	c	0.2892113	18.12	0.08	18.06	0.10	18.07	0.04
OGLE051824.42-690459.4	ab	0.6464268	18.28	0.06	17.95	0.07	17.99	0.09
OGLE051834.72-690550.6	ab	0.4991066	18.20	0.06	17.99	0.08	18.07	0.02
OGLE051835.56-690406.0	ab	0.4736237	18.22	0.08	18.18	0.09	18.19	0.10
OGLE051836.59-690839.6	ab	0.5336746	18.55	0.09	18.47	0.05	18.38	0.05
OGLE051836.68-690659.7	ab	0.5913999	18.27	0.07	18.10	0.04	18.03	0.04
OGLE051837.86-690821.3	c	0.2873557	18.79	0.09	18.57	0.12	18.57	0.00
OGLE051841.62-690609.4	ab	0.7517683	18.27	0.05	17.84	0.07	17.81	0.01
OGLE051842.24-690724.5	ab	0.6597547	18.28	0.03	17.94	0.03	17.94	0.03
OGLE051843.33-690502.6	ab	0.5676291	18.37	0.07	18.11	0.09	18.13	0.02
OGLE051853.07-690819.5	ab	0.5805700	18.30	0.04	17.93	0.06	18.00	0.06
OGLE051923.06-693859.0	ab	0.6438395	18.36	0.07	17.79	0.10	17.84	0.01
OGLE052301.40-700731.0	c	0.2964723	18.58	0.05	18.39	0.05	18.39	0.05
OGLE052308.89-700746.7	c	0.3425135	18.48	0.05	18.24	0.05	18.24	0.05
OGLE052317.13-700607.2	ab	0.6020069	18.33	0.08	18.10	0.08	18.05	0.08
OGLE052318.43-700651.5	ab	0.5521760	18.33	0.05	17.96	0.04	18.00	0.04
OGLE052321.67-700739.9	ab	0.5214616	18.41	0.06	18.35	0.04	18.24	0.04
OGLE052328.70-700523.8	c	0.3728943	17.96	0.09	17.78	0.10	17.77	0.05
OGLE052329.54-700713.1	ab	0.6590143	18.06	0.09	17.71	0.06	17.75	0.04
OGLE052331.40-700529.1	ab	0.6131165	18.02	0.09	17.78	0.08	17.85	0.05
OGLE052332.28-700654.1	ab	0.6235510	17.36	0.06	17.28	0.06	17.31	0.00
OGLE052335.14-700505.4	ab	0.5072454	18.30	0.07	18.10	0.09	18.07	0.01
OGLE052340.40-700639.8	ab	0.5148516	18.04	0.07	18.07	0.08	18.10	0.08
OGLE052341.81-700632.4	ab	0.5285457	18.84	0.12	18.56	0.12	18.64	0.20
OGLE052345.86-700504.2	ab	0.5711875	18.10	0.07	17.95	0.09	17.88	0.05
OGLE052349.66-700327.1	ab	0.6631955	18.17	0.12	18.03	0.12	18.04	0.11
OGLE052350.37-700443.2	ab	0.5054740	18.53	0.10	18.24	0.11	18.26	0.04

Table 5—Continued

Star ID	Star type	Period [days]	J	σ	K	σ	$\langle K \rangle$	σ
OGLE052353.56-700432.4	ab	0.5520142	18.31	0.07	18.13	0.08	18.21	0.13
OGLE052355.34-700802.6	c	0.2628732	18.77	0.11	18.67	0.19	18.56	0.14
OGLE052357.93-700322.9	ab	0.5125914	18.80	0.08	18.54	0.18	18.47	0.06
OGLE052400.52-700520.9	ab	0.5816737	18.40	0.06	18.05	0.08	18.04	0.02
OGLE052405.11-700611.5	ab	0.5950911	18.23	0.07	17.96	0.08	17.93	0.05
OGLE052418.64-700307.7	c	0.3354890	18.28	0.11	18.18	0.16	18.18	0.16
OGLE052419.91-700616.7	ab	0.5036958	...	...	17.90	...	17.83	...
OGLE052423.93-700736.4	ab	0.5816925	18.32	0.05	18.12	0.04	17.93	0.04
OGLE052859.00-700822.2	ab	0.5515840	18.97	0.10	18.31	0.13	18.08	0.13
OGLE052909.42-700828.1	ab	0.9210850	17.70	0.05	17.42	0.07	17.31	0.07
OGLE052911.54-700836.5	ab	0.5469046	18.58	0.06	17.99	0.07	17.99	0.07
OGLE052917.43-700734.5	ab	0.6015387	18.34	0.04	18.06	0.07	18.12	0.07
OGLE052917.77-700535.6	ab	0.7286710	18.43	0.07	17.81	0.07	17.68	0.07
OGLE052917.87-700841.1	ab	0.4802590	18.54	0.05	18.23	0.08	18.15	0.08
OGLE052917.92-700712.2	c	0.3383890	18.51	0.07	18.06	0.10	18.06	0.10
OGLE052929.39-700551.0	ab	0.6215635	18.00	0.04	17.59	0.06	17.65	0.06
OGLE052932.88-700842.3	ab	0.5442339	18.37	0.06	18.26	0.09	18.27	0.09
OGLE052933.54-700715.9	ab	0.5340639	18.58	0.05	18.03	0.08	17.99	0.08
OGLE052936.94-700721.1	ab	0.5858587	18.37	0.05	18.35	0.08	18.34	0.08
OGLE052937.91-700844.9	c	0.3758092	18.24	0.05	17.95	0.08	17.95	0.08
OGLE052949.93-700558.2	ab	0.5625618	18.66	0.06	18.22	0.09	18.17	0.09
OGLE053147.30-694349.6	ab	0.5074034	18.11	0.05	17.82	0.07	17.90	0.07
OGLE053147.82-694142.2	ab	0.6455259	18.05	0.05	17.81	0.07	17.70	0.07
OGLE053155.92-694232.4	ab	0.5211680	18.35	0.05	18.19	0.08	18.17	0.08
OGLE053200.94-694219.1	ab	0.6062906	18.20	0.09	18.01	0.12	17.95	0.12
OGLE053203.62-694210.7	ab	0.4796139	18.26	0.04	17.99	0.07	18.05	0.07
OGLE053206.72-694342.1	ab	0.5192097	18.51	0.04	18.38	0.09	18.42	0.09
OGLE053206.78-694224.7	ab	0.5230170	17.98	0.04	18.02	0.07	18.04	0.07
OGLE053207.32-694117.2	ab	0.5626089	17.76	0.03	17.53	0.06	17.58	0.06
OGLE053207.88-694058.7	ab	0.6218200	18.15	0.04	17.93	0.07	18.02	0.07

Table 5—Continued

Star ID	Star type	Period [days]	J	σ	K	σ	$\langle K \rangle$	σ
OGLE053217.55-694317.6	ab	0.5485307	17.95	0.05	17.87	0.07	17.87	0.07
OGLE053219.15-694215.2	ab	0.6521316	18.22	0.05	17.94	0.07	17.97	0.07
OGLE053222.39-693952.9	ab	0.6769293	18.23	0.07	18.03	0.11	18.10	0.11
OGLE053225.42-694438.2	ab	0.6427599	18.38	0.07	18.03	0.12	18.07	0.12
OGLE053229.21-694411.0	ab	0.5960780	...	...	18.15	0.09	18.10	0.09

Table 6. PL relations determined for averaged data

Data set	J slope	J zeropoint	K slope	K zeropoint
RRab+RRc				
Free fit	-1.381±0.468	17.953±0.123	-2.192±0.399	17.493±0.108
Sollima et al. (2008)	...	...	-2.380	17.443±0.026
Bono et al. (2003)	...	...	-2.101	17.516±0.026
Catelan et al. (2004)	-1.773	17.850±0.030	-2.353	17.450±0.026
RRab				
Sollima et al. (2008)	...	...	-2.380	17.463±0.029
Bono et al. (2003)	...	...	-2.101	17.531±0.029
Catelan et al. (2004)	-1.773	17.869±0.033	-2.353	17.469±0.029

Table 7. PL relations determined for mean data, using the light-curve templates

Data set	K slope	K zeropoint
RRab+RRc		
Sollima et al. (2008)	-2.380	17.421±0.026
Bono et al. (2003)	-2.101	17.500±0.026
Catelan et al. (2004)	-2.353	17.434±0.026
RRab		
Sollima et al. (2008)	-2.380	17.445±0.029
Bono et al. (2003)	-2.101	17.512±0.029
Catelan et al. (2004)	-2.353	17.451±0.029

Table 8. Determined true distance moduli for different data sets and PL relations.

Data set	Sollima et al. (2008)	Bono et al. (2003)	Catelan et al. (2004)
RRab+RRc (J)	...	...	18.546 ± 0.026
RRab+RRc (K)	18.580 ± 0.026	18.621 ± 0.026	18.607 ± 0.026
RRab (J)	...	...	18.565 ± 0.029
RRab (K)	18.600 ± 0.029	18.620 ± 0.029	18.611 ± 0.029
RRab+RRc ($\langle K \rangle$)	18.564 ± 0.026	18.604 ± 0.026	18.590 ± 0.026
RRab ($\langle K \rangle$)	18.582 ± 0.029	18.617 ± 0.029	18.608 ± 0.029